NUMERICAL INVESTIGATION OF A THREE-DIMENSIONAL DISC-PAD MODEL WITH AND WITHOUT THERMAL EFFECTS

by

Ali BELHOCINE *

Faculty of Mechanical Engineering, University of Sciences and Technology of Oran, El-Mnaouer, Oran, Algeria

Original scientific paper
DOI: 10.2298/TSCI141130072B

This study aims to identify thermal effects in the structure and the contact behavior of a disc-pad assembly using a finite element approach. The first analysis is performed on the disc-pad model in the absence of thermal effects. The structural performance of the disc-pad model is predicted in terms of factors such as the deformation and Von Mises stress. Thermo-mechanical analysis is performed on the same disc-pad model with the inclusion of convection, adiabatic, and heat flux elements. The predicted temperature distribution, deformation, stress, and contact pressure are presented. The structural performance between the two analyses (mechanical and thermo-mechanical) is compared. This study can assist brake engineers in choosing a suitable analysis method to critically evaluate the structural and contact behavior of the disc brake assembly.

Key words: *finite element, disc-pad model, temperature, deformation, stress, contact pressure*

Introduction

During basic operation, a disc or drum brake system has to reduce the wheel speed when a driver desires vehicle deceleration. The kinetic energy generated by a vehicle in terms of wheel speed is converted into heat energy owing to the application of the brake system. The energy transforming process takes place entirely on contact surfaces of disc and friction linings of brake pads. The heat is carried out on this way transfers threw the parts in contact (disc and brake pad) at first, by means of conductivity and after that, dissipate into the surroundings, by convection and radiation [1].

Ji *et al.* [2] investigated the temperature, stress and plastic deformation of wet multidisc brake when material properties are temperature-dependent using finite element analysis for bidirectional thermal-structure coupling. Belhocine and Bouchetara [3] used numerical simulation to study the thermo-mechanical analysis of brake disk with a grey cast iron composition. Rajagopal *et al.* [4] studied the effect of vane-shape on the flow-field and heat transfer characteristics for different configurations of vanes and at different speeds numerically. The predicted results have been validated with the results available in the literature. Milošević *et al.* [5] have carried out the thermal analysis of a braking system of railway vehicles using analytical

Authors' e-mail: al.belhocine@yahoo.fr

and numerical modeling of thermal effects during long-term braking for maintaining a constant speed on a down-grade railroad in order to analyze damages of solid wheels braked by blocks, especially on railway vehicles. Duzgun [6] did a study on the investigation of thermo-structural behaviors of different ventilation applications on brake discs. Pevec *et al.* [7] have studied the prediction of the cooling factors of a vehicle brake disc and its influence on the results of a thermal numerical simulation. Jung *et al.* [8] have studied thermal characteristic analysis and shape optimization of a ventilated disc. Hwang and Wu [9] have studied the investigation of temperature and thermal stress in ventilated disc brake based on 3-D thermo-mechanical coupling model. Pharande and Pawar [10] conducted a study in order to investigate the temperature and thermal stress in the ventilated disc-pad brake during single brake. The brake disc is decelerated at the initial speed with constant acceleration, until the disc comes to a stop. The ventilated pad-disc brake assembly is built by a 3-D model with a thermo-mechanical coupling boundary condition and multi-body model technique.

The present study aimed to investigate the structural and contact behaviors of the brake disc and pads during the braking phase with and without thermal effects. First, the total deformation of the disc-pad model at the time of braking and the stress and contact distributions of the brake pads were determined. Then, the results of thermoelastic coupling, such as Von Mises stress, contact pressure field, and total deformations of the disc and pads, were presented. These will be useful in the brake design process for the automobile industry.

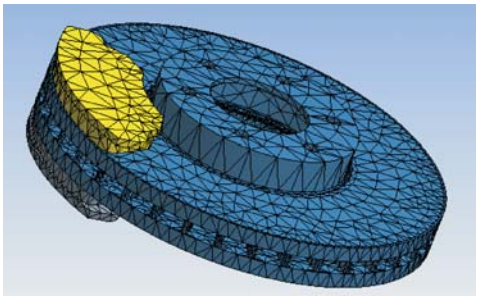

Figure 1. The FE model of a disc-pad assembly

Finite element model

In this study, a 3-D finite element (FE) model consisting of a ventilated disc and two pads is employed, as illustrated in fig. 1.

The disc is made of gray cast iron FG 15 with high carbon content and the brake pad in semi-metallic steel fibers shows isotropic elastic behavior. Table 1 lists the mechanical characteristics of these two parts. The thermal conductivity and specific heat are a function of temperature, figs. 2 and 3.

The ANSYS 11 (3-D, commercial FE software is used fully utilized to simulate the structural deformation, stress, temperature, and contact pressure distributions of the disc brake during braking. Coupled transient thermal and structural static analysis are done on the disc-pad model, that do not induce significant inertia and damping effects. The static frictional coefficient is assumed to be constant in this analysis.

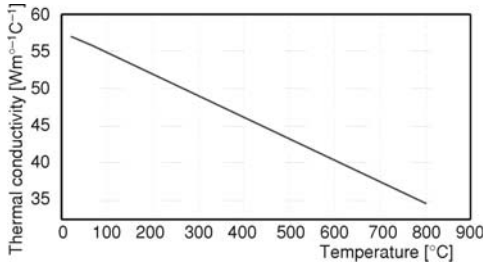

Figure 2. Thermal conductivity as a function of temperature

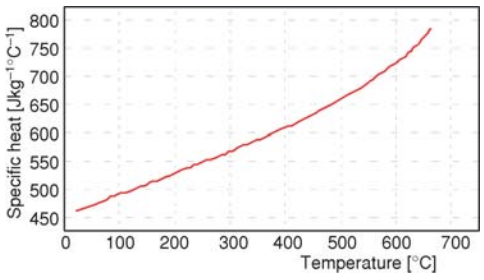

Figure 3. Specific heat *vs.* temperature

Determination of hydraulic pressure

In this study, the initial mechanical calculation aims at determining the value of the contact pressure (presumably constant) between the disc and the pad. It is assumed that 60% of the braking forces are supported by the front brakes (both discs), *i. e.*, 30% for a single disc, as cited in [11]. The force of the disc for a typical vehicle is calculated using the vehicle data listed in tab. 2, to obtain the working forces on the brake disc:

$$F_{\text{disc}} = \frac{(30\%)\frac{1}{2}Mv_0^2}{2\frac{R_{\text{rotor}}}{R_{\text{tire}}}\left[v_0 t_{\text{stop}} - \frac{1}{2}\left(\frac{v_0}{t_{\text{stop}}}\right)t_{\text{stop}}^2\right]} \quad (1)$$

The rotational speed of the disc is calculated:

$$\omega = \frac{v_0}{R_{\text{tire}}} \quad (2)$$

The total disc surface in contact with the pads is 35797 mm^2, as shown in fig. 4.

The hydraulic pressure is obtained using eq. (1) as mentioned in [12]:

Table 1. Thermo-elastic properties of the disc and pad

	Disc	Pad
Young modulus, E [GPa]	138	1
Poisson's ratio, υ	0.28	0.25
Density, ρ [kgm^{-3}]	7250	1400
Coefficient of friction, μ	0.2	0.2
Thermal conductivity, k [Wm^{-1}°C]	57	5
Thermal expansion, α [10^{-6}°C]	10.85	10
Specific heat, c [Jkg^{-1}°C]	460	1000
Angular velocity, ω [rads^{-1}]	157.89	
Hydraulic pressure, P [MPa]	1	

Table 2. Vehicle data

Vehicle mass, M [kg]	1385
The initial velocity, v_0 [ms^{-1}]	60
Duration of braking application, t_{stop} [s]	45
The effective radius of the disc [mm]	100.5
The radius of the wheel [mm]	380
Friction coefficient disc/pad, μ [–]	0.2
Pad surface, A_{d} [mm^2]	5246.3
Rotor force, F_{disc} [N]	1047.36

$$P = \frac{F_{\text{disc}}}{A_c \mu} \quad (3)$$

where A_c is the surface area of the pad in contact with the disc and μ – the friction coefficient. The surface area of the pad in contact with the disc in mm^2 is given directly in ANSYS by selecting this surface, as indicated by the green color in fig. 5. For a brake pad without a groove, the hydraulic pressure is calculated in the same manner.

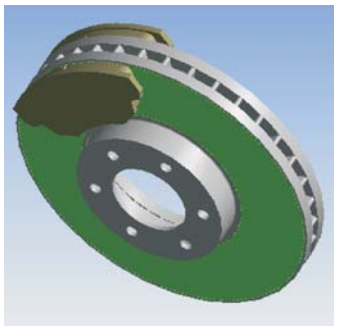

Figure 4. Contact surface of the disc

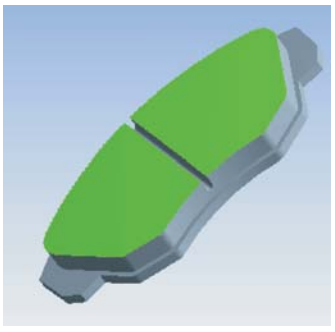

Figure 5. Contact surface of the pad

Boundary conditions and loading of the disc and pads

In this FE model, boundary conditions are imposed on the models (disc-pad) as shown in figs. 6(a) and 6(b), respectively, for applied pressure on one and both sides of the pad. The inner and outer pad, respectively, rides on the inside and outside of the brake rotor. The disc is rigidly constrained at the bolt holes in all directions except in its rotational direction. Meanwhile, the pad is fixed at the abutment in all degrees of freedom except in the normal direction to allow the pads to move up and down and in contact with the disc surface [13].

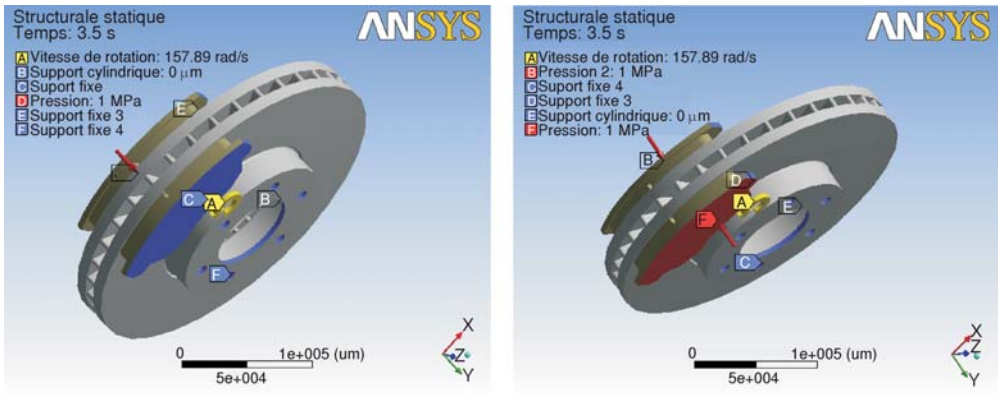

(a) One side (b) Two sides

Figure 6. Boundary conditions and loading imposed on the disc-pads

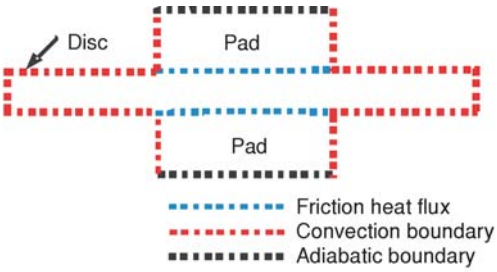

Figure 7. Boundary condition for thermal analysis of the disc brake

Thermal boundary conditions

To express the heat transfer in the disc brake model, the thermal boundary conditions and initial condition have to be defined. At the interface between the disc and the brake pads, heat is generated owing to sliding friction, as indicated by the dashed in fig. 7. In the exposed region of the disc and brake pads, it is assumed that heat is exchanged with the environment through convection, as cited in [14]. Therefore, the convection surface boundary condition is applied there. On the surface of the back plate, an adiabatic or insulated surface boundary condition is used and shown in fig. 7.

Finite element results and discussion

Disc-pad model without thermal effects

The computer code ANSYS also allows the determination and visualization of the structural deformations owing to the sliding contact between the disc and the pads. The results of the calculations of the contact described in this section relate to displacements or the total deformation during the loading sequence, the field of equivalent Von Mises stress on the disc, and the contact pressures of the inner and outer pads at different braking periods.

Disc-pad deformation

Figures 8(a)-8(c) show the disc deformations against the braking time. It is noted that large deformation is always found at the outer radius of the disc; this is the area in contact with the pad. These figures show that the highest deformation is 53 μm, and it is predicted at a braking time of t = 3.5 s and onwards. For pads, the highest deformation is located at the outer radial region (visualized in red), as shown in fig. 9. Furthermore, the pads are less deformed compared to the disc, as shown in fig. 10. At a braking time of t = 3.5 s and onwards, the maximum deformation of the pads is predicted to be 19 μm, which is 64% lower than that of the disc. This is due to the structural stiffness and type of constraints that have been assigned to the disc and pads.

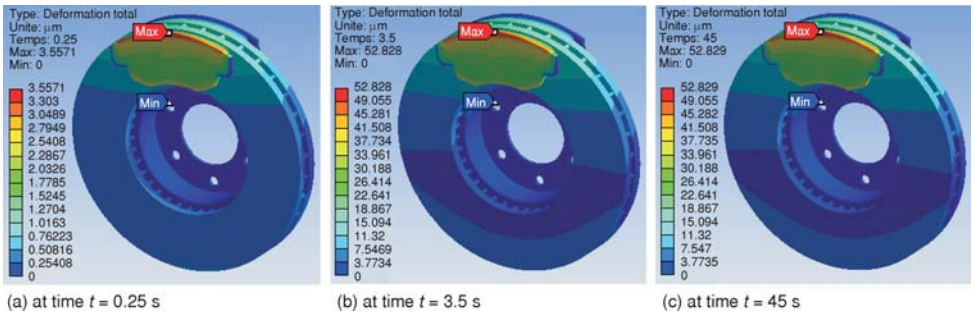

Figure 8. Disc deformation at different braking time

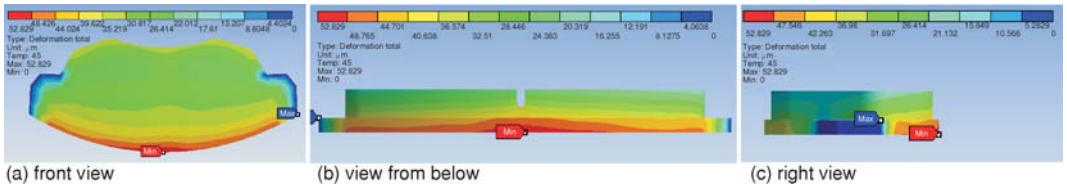

Figure 9. Pad deformation at braking time t = 45 s

For the effects without thermal influence, the deformations located in the mean and outer radius of the disc at different angular positions (θ) are given in fig. 11. It is noted that the two curves follow the same pattern. The highest deformation is predicted at an angular position of 90° which corresponds to the position of tightening of the disc by the pads. Deformations behavior with rotation is completely in conformity with the observations usually made with the brake discs.

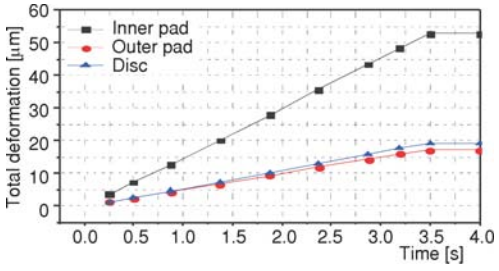

Figure 10. Deformation of the disc and pads at different braking period

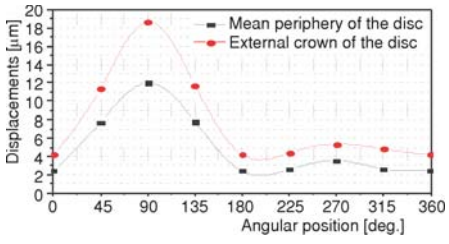

Figure 11. Disc deformation at the mean and outer radius over angular positions at braking time t = 3.5 s

Stress distribution of pad

Figures 12(a)-12(c), show that the equivalent Von Mises stress is distributed almost symmetrically between the leading and the trailing side of the pad. These stress distributions are barely unchanged over braking time, except for the stress value. The stress increases gradually and reaches its maximum value of 5.3 MPa at a braking time of 3.5 s and onwards. The highest

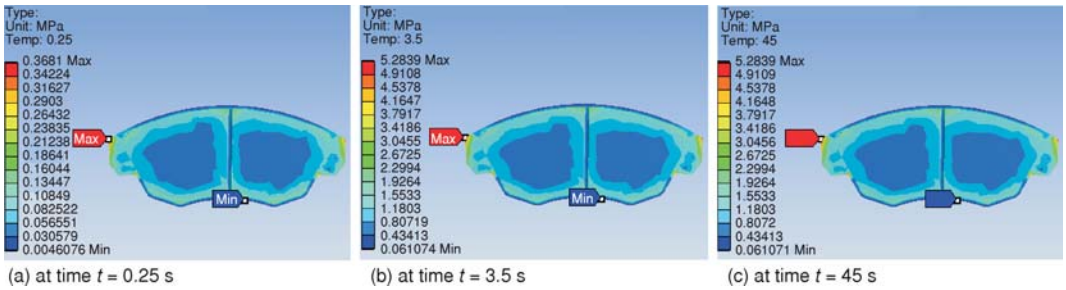

Figure 12. Von Mises stress distribution of the pad over braking time

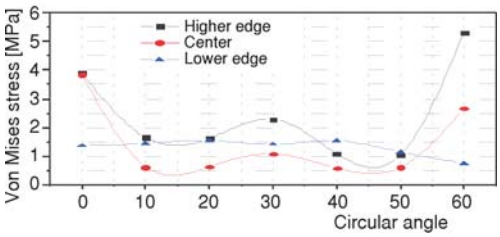

Figure 13. Von Mises stress at different angular positions of the pad

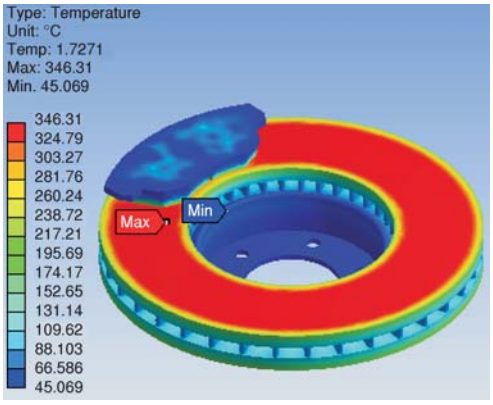

Figure 14. Temperature distribution of the disc and pads at braking time

stress is predicted on the left side and the outer radius of the pad, whereas the lowest stress is located on the lower radius of the pad and near the groove area. Figure 13 shows a clear picture of the stress distributions at a braking time of t = 45 s across the inner pad contact surface. More uniform stress distribution occurs at the lower radius of the pad compared to the outer radius and center region of the pad. In addition, the highest stress is generated on the right and left sides at the outer radius and center region of the pad, respectively.

Disc-pad model with thermal effect

Structural and thermal analyses are coupled using ANSYS multiphysics to identify the stress levels and global deformations of the model studied during the braking phase under the effect of temperature.

Temperature distribution

The initial temperature of the disc and pads is set at 20°, surface convection condition is applied to all surfaces of the disc, and convection coefficient of 5 W/m^2°C is applied at the surface of the two pads. Figure 14 shows that at a braking time of 1.7 s, the disc and pad surface generates a very high temperature, of 346 °C.

Thermal conductivity and thermal stability play a vital role in the performance of brake pads. In our case, steel fiber a semi-metallic composition has good thermal stability and bulk density. The temperature rise during brake application will be between 150-400 °C. However, the upper part of the back plate shows a lower temperature of 90 °C. This is caused by the convection of ambient air.

Deformation and Von Mises stress of disc-pad model

The aim of this coupled structural-thermal analysis, is to gain a better understanding of the total deformation of the disc when it is not only subjected to loading from the pads but also the expansion induced by the effect of temperature. Figure 15 shows the disc deformations at the nodes located in the mean and outer radius of the disc. A clear difference in disc deformation can be found between these two regions, where the outer radius of the disc shows higher deformation than the mean radius. The curves indicate an umbrella phenomenon that results from the heating of non-parallel paths of friction with respect to the initial position. Figure 16 shows that the disc deformation increases linearly as a function of the disc radius. The highest deformation is predicted at an angular position of 90° and the lowest deformation, at 270°.

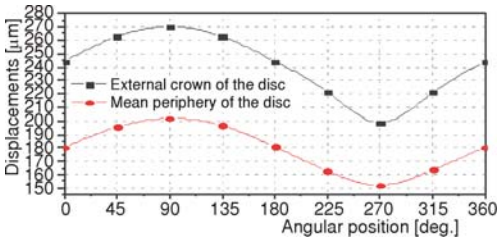

Figure 15. Disc deformation at the mean and outer radius over angular positions at braking time t = 3.5 s

Comparing the different results of deformation rise, obtained from analysis according to figs. 11 and 15. The total deformations of the disc-pad model increase in a notable way, when we place in a coupled thermo-mechanical aspect.

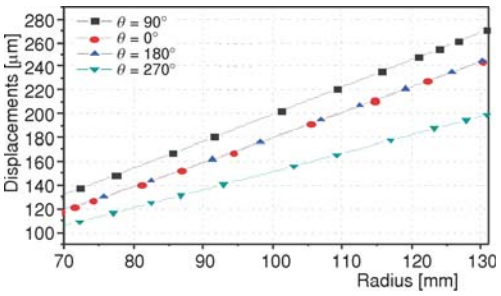

Figure 16. Disc deformation at different radius and angular positions at braking time t = 3.5 s

The result shows that there is a significant difference between the mechanical and the thermo-elastic model in terms of deformation and contact pressure. Figure 17 shows that the disc deforms severely under the effect of temperature. For instance, at braking time of 3.5 s, the discs with and without the thermal effect deforms by 280 and 53 μm, respectively. This clearly indicates that temperature strongly influences the thermo-mechanical response of the brake disc. During a braking maneuver, the maximum temperature achieved on the tracks depends on the storage capacity of the thermal energy in the disc. Figure 18, shows that the maximum displacement is localized on the slopes of friction, fins, and outer ring. This phenomenon is due to the fact that the deformation of the disc is caused by heat (umbrella effect) that can lead to cracking of the disc. In this case,

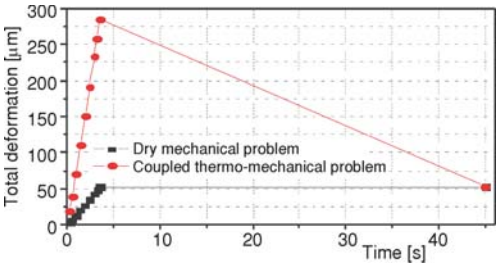

Figure 17. Disc deformation with and without thermal effects

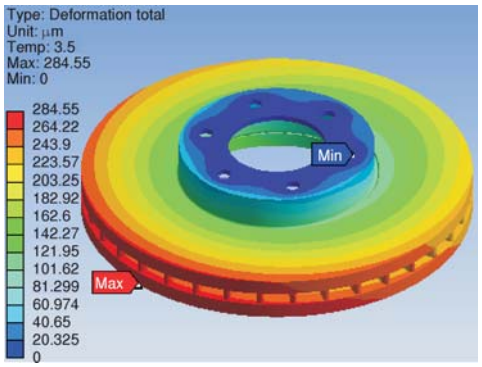

Figure 18. Maximum total deformation of the disc with thermomechanical coupling

thermo-coupling analysis is quite important to determine where thermal gradients and expansions generate thermal stresses in addition to the mechanical stress.

Von Mises stress at inner pad

The influence of the pad groove and loading modes (single and dual piston) on the equivalent Von Mises stress distribution is presented. Figures 19(a)-19(c) show the stress evolution for three pad designs. At the beginning of braking (t = 1.7 s), most of the pad contact surfaces are dark blue, indicating lower stress. However, by a braking time of t = 45 s, the stress level in-

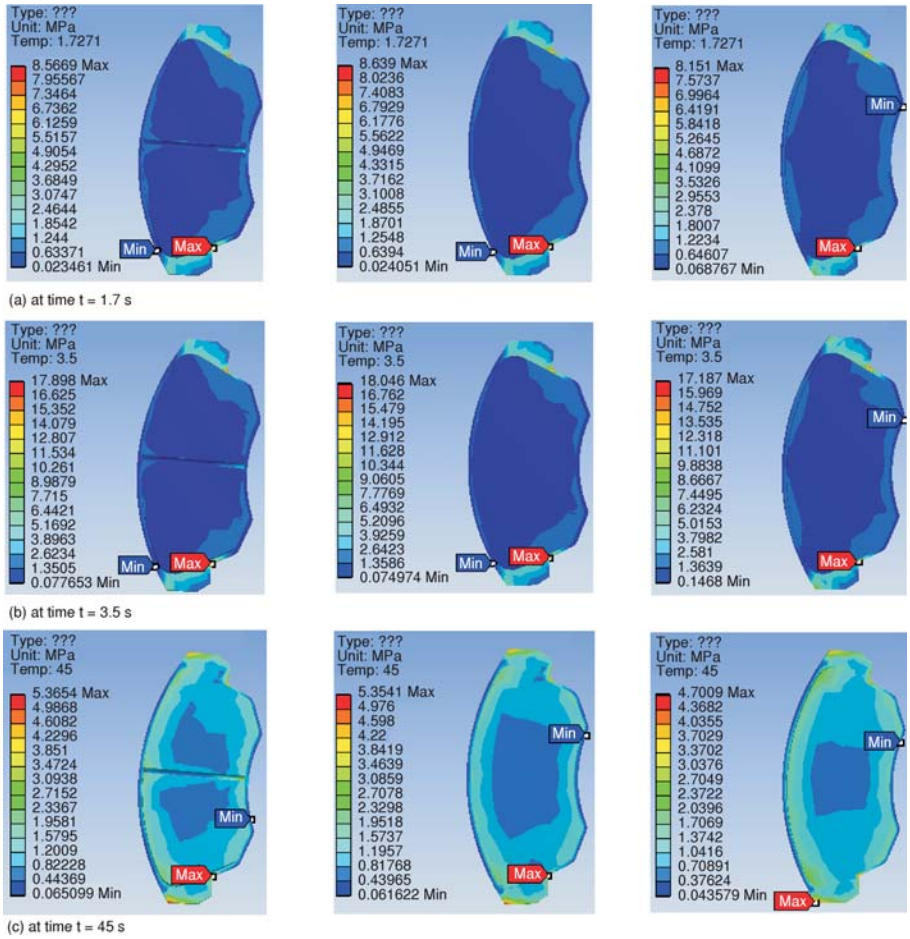

Figure 19. Distribution of Von Mises stress at different braking time: single piston with pad center-groove (left), single piston without groove (center), and double piston without pad groove (right)

creases and the color becomes almost ocean blue. At this braking time, the three pad designs clearly show different stress distributions. The presence of the groove and double piston loading has a positive effect on the stresses of the pad.

Contact pressure distribution

The contact pressure distribution plotted in fig. 20 is based on a braking time of t = 3.5 s, where the pad surface temperature is T = 346 °C. It is seen that the contact pressure curves are almost identical in shape for three different regions of the pad. At 30° angle, the contact pressure is predicted to be higher at lower pad radius followed by the outer pad radius and middle pad radius. The most significant outcome is to see the effect of temperature on the contact pressure of the disc-pad model. Figure 21, shows the significant variation of the two curves. The contact pressure distribution of the pads increases remarkably, when the thermal and mechanical aspects are coupled. This gives an indication to brake engineers that in order to evaluate the brake performance, thermo-mechanical analysis should first be performed so that a realistic prediction can be achieved.

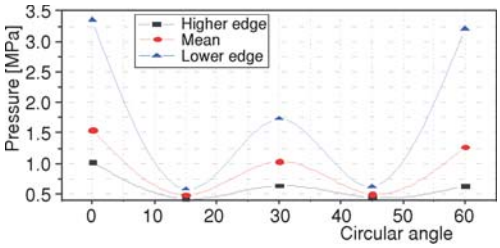

Figure 20. Distribution of contact pressure along the lower, middle, and upper radius of the pad at time t = 3.5 s

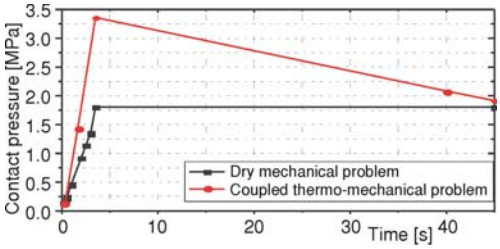

Figure 21. Contact pressure of the inner pad

Conclusions

In this study, a disc-pad model has been analyzed using two approaches, namely, mechanical and thermo-mechanical analysis. In addition, three pad designs have been simulated to identify its influence on the stress distribution. From the prediction results, the following conclusions can be derived.

- Large deformation occurs at the outer radius of the disc.
- More uniform stress distribution is observed for a pad without groove and with double-piston loading.
- Temperature significantly affects the structural and contact behavior of the disc brake assembly. Large deformation and high contact pressure are observed in the disc-pad model with the thermal effect.

Based on the findings of this study, the following issues can be considered for further study:

– experimental study to verify the accuracy of the numerical model developed.
– tribology and vibrations study of contact disc-pads, and
– dry contact sliding under macroscopic aspects (macroscopic state of the surface of disc and pads).

Nomenclature

A_c – surface area of the pad in contact with the disc, [mm^2]
A_d – pad surface, [mm^2]
c – specific heat, [Jkg^{-1}°C^{-1}]
E – Young modulus, [GPa]
F_{disc} – rotor force, [N]

k – thermal conductivity, [$Wm^{-1}°C^{-1}$]
M – vehicle mass, [kg]
P – hydraulic pressure, [MPa]
R – radius, [mm]
t_{stop} – time to stop, [s]
v_0 – initial velocity, [ms^{-1}]

Greek symbols

α – thermal expansion, [$10^{-6}°C^{-1}$]
μ – static friction coefficient
ρ – density, [kgm^{-3}]
υ – Poisson's ratio

References

[1] Milenković, P. D., *et al.*, The Influence of Brake Pads Thermal Conductivity on Passanger Car Brake System Efficiency, *Thermal Science, 14* (2010), Suppl. 1, pp. S221-S230
[2] Ji, Z., *et al.*, Elastoplastic Finite Element Analysis for Wet Multidisc Brake during Lasting Braking, *Thermal Science, 19* (2015), 5, pp. online first, doi:10.2298/TSCI141121016J
[3] Belhocine, A., Bouchetara, M., Thermomechanical Behaviour of Dry Contacts in Disc Brake Rotor with a Grey Cast Iron Composition, *Thermal Science, 17* (2013), 2, pp. 599-609
[4] Rajagopal, T. K. R., *et al.*, Numerical Investigation of Fluid Flow and Heat Transfer Characteristics on the Aerodynamics of Ventilated Disc Brake Rotor Using CFD, *Thermal Science, 18* (2014), 2, pp. 667-675
[5] Milošević, M. S., *et al*., Modeling Thermal Effects in Braking Systems of Railway Vehicles, *Thermal Science, 16* (2014), 2, pp. 515-526
[6] Duzgun, M., Investigation of Thermo-Structural Behaviors of Different Ventilation Applications on Brake Discs, *Journal of Mechanical Science and Technology, 26* (2012), 1, pp. 235-240
[7] Pevec, M., *et al*., Prediction of the Cooling Factors of a Vehicle Brake Disc and its Influence on the Results of a Thermal Numerical Simulation, *International Journal of Automotive Technology, 13* (2012), 5, pp. 725-733
[8] Jung, S. P., *et al*., A Study on Thermal Characteristic Analysis and Shape Optimization of a Ventilated Disc, *International Journal of Precision Engineering and Manufacturing, 13* (2012), 1, pp. 57-63
[9] Hwang, P., Wu, X., Investigation of Temperature and Thermal Stress in Ventilated Disc Brake Based on 3D Thermomechanical Coupling Model, *Journal of Mechanical Science and Technology, 24* (2010), 1, pp. 81-84
[10] Pharande, R. D., Pawar, S. G., Study of the Thermo-Mechanical Behaviour of Dry Contacts in the Brake Discs with a Grey Cast Iron Composition (FG260), Application of Software Ansys V13.0, *International Journal of Engineering Research & Technology, 2* (2013), 3, pp. 1-6
[11] Mackin., T. J., *et al.*, Thermal Cracking in Disc Brakes, *Engineering Failure Analysis, 9* (2002), 1, pp. 63-76
[12] Oder, G., *et al.*, Thermal and Stress Analysis of Brake Discs in Railway Vehicules, *Advanced Engineering, 3* (2009), 1, pp. 95-102
[13] Coudeyras, N., Non-Linear Analysis of Multiple Instabilities to the Rubbing Interfaces: Application to the Squealing of Brake, Ph. D. thesis, Central School of Lyon-Speciality: Mechanics, Lyon, France, 2009
[14] Sarip, S. B., Lightweight Friction Brakes for a Road Vehicle with Regenerative Braking, Ph. D. thesis, Engineering Design and Technology, Bradford University, Bredford, UK, 2011

Paper submitted: November 30, 2014
Paper revised: May 3, 2015
Paper accepted: May 25, 2015